# Severe creep of a crystalline metallic layer induced by swift-heavy-ion irradiation

F. Garrido
*Centre de Spectrométrie Nucléaire et de Spectrométrie de Masse, IN2P3-CNRS, Bât. 108, F-91405 Orsay Campus, France*

A. Benyagoub
*Institut de Physique Nucléaire de Lyon, IN2P3-CNRS et Université Claude-Bernard, 43 Bd du 11 Novembre 1918, F-69622 Villeurbanne Cedex, France*

A. Chamberod
*Département de Recherche Fondamentale, Centre d'Etudes de Grenoble, F-38041 Grenoble, France*

J.-C. Dran
*Centre de Spectrométrie Nucléaire et de Spectrométrie de Masse, IN2P3-CNRS, Bât. 108, F-91405 Orsay Campus, France*

A. Dunlop
*CEA Laboratoire des Solides Irradiés, Ecole Polytechnique, F-91128 Palaiseau Cedex, France*

S. Klaumünzer
*Hahn-Meitner-Institut, Glienicker Straße 100, D-14109 Berlin, Germany*

L. Thomé
*Centre de Spectrométrie Nucléaire et de Spectrométrie de Masse, IN2P3-CNRS, Bât. 108, F-91405 Orsay Campus, France*
(Received 3 March 1995)

The aim of the experiments presented in this paper was to study the mechanisms leading to the atomic transport process (plastic deformation) induced in amorphous solids by GeV heavy-ion irradiation. $Ni_3B/Au/Ni_3B$ sandwiches, composed of a crystalline Au layer of various thicknesses and of two amorphous $Ni_3B$ layers, were irradiated at liquid nitrogen temperature with 500-MeV iodine ions. The Rutherford backscattering technique using a 3.6-MeV He beam was applied to determine the modifications of the geometry of the sandwiches due to irradiation. The results show a radiation-induced creep of the crystalline layer, with a strain-rate decreasing with increasing layer thickness. This creep phenomenon is due to the plastic deformation process occurring in the surrounding amorphous layers, and is induced by ion electronic energy loss. A simple rheological model is developed to quantify the observed effects.

## I. INTRODUCTION

Ion bombardment of a solid target is responsible for a great variety of atomic movements due to (i) elastic collisions between the projectile and target nuclei (nuclear energy loss), dominant at low ion energy ($< \sim 10$ keV/u), and (ii) excitation and ionization of target atoms (electronic energy loss), dominant at very high ion energy ($> \sim 1$ MeV/u). The former process leads to the formation of displacement cascades in all kinds of solids, and generates the well-known ion-beam-mixing phenomenon. For a long time the study of electronic energy loss effects in solids was performed by using fission fragments. Most studies were restricted to insulators, in which the formation of so-called "latent tracks" was early discovered.[1] At the beginning of the 1980s the advent of facilities allowing one to accelerate heavy ions at energies in the GeV range brought a new impetus in the field of particle-solid interaction by the discovery of unexpected effects of electronic energy loss in metallic systems.[2] In this respect, one of the most dramatic manifestations of atomic motion induced by electronic excitation is the plastic deformation evidenced in amorphous materials irradiated with swift heavy ions.[3]

This long-range atomic transport phenomenon, which consists of a growth of the dimensions of the target perpendicular to the ion beam direction together with a shrinkage of the dimension parallel to it (so that the volume of the sample remains constant), was first macroscopically studied by length[3-7] and electrical resistance measurements.[8-10] Later on, investigations at a lower scale, conducted by means of nuclear microanalysis associated with a heavy marker implanted in the surface region of the irradiated target, demonstrated that the plastic deformation process sensed at a mesoscopic scale is identical to the global process.[11] It was then particularly interesting to extend this investigation to the case of an amorphous solid containing a crystalline bulky layer with the double purpose (i) to sense the deformation of the various (amorphous as well as crystalline) layers by nuclear microanalysis, and (ii) to hamper the plastic deformation of the amorphous layer via long-range elastic forces. In other words, the use of crystalline layers of variable thicknesses allows one to study the competition

0163-1829/95/52(9)/6273(5)/$06.00  

between the local plastic deformation generated by individual ion impacts in the amorphous regions and long-range macroscopic elastic forces arising from the crystalline part of the target, in order to provide a better insight on the processes which allow one to convert electronic excitation into atomic movements. This study was done by the measurement, with the Rutherford backscattering (RBS) technique, of the spatial modifications (due to swift-heavy-ion irradiation) of a crystalline marker layer of different thicknesses sandwiched between two amorphous layers of the investigated system.

The experiments reported in this paper have allowed us to evidence, and also to quantify, a severe creep phenomenon experienced by a pure crystalline metallic layer submitted to ion beam-induced electronic excitation.

## II. EXPERIMENT

The targets consist of $Ni_3B/Au/Ni_3B$ sandwiches composed of a crystalline Au layer of thickness varying from 30 to 900 nm and of two amorphous $Ni_3B$ layers of thickness 1.0 or 1.5 $\mu$m. They were prepared by sputtering at the Centre d'Etudes de Grenoble.

The samples were partly clamped between two copper plates and irradiated at normal incidence over an area of $2\times3$ mm$^2$ at liquid nitrogen temperature with 500-MeV $^{127}I^{22+}$ ions delivered by the VICKSI accelerator of the Hahn-Meitner-Institut in Berlin.[12] The ion fluences $\Phi$ range from 1 to $3\times10^{13}$ at cm$^{-2}$. The total thickness of the sandwiches is much less than the ion projected range so that the iodine ions are not implanted into the target. The flux $\varphi$ was always kept below $10^9$ ions cm$^{-2}$ s$^{-1}$ in order to avoid excessive heating of the samples during irradiation. The average value of electronic energy loss is $\sim$40 keV/nm.

The analysis of the modifications of the sample geometry along the ion beam direction (thickness of the $Ni_3B$ and Au layers) was performed before and after irradiation by conventional RBS experiments with a 3.6-MeV $^4He^{2+}$ beam provided by the ARAMIS accelerator of the Centre de Spectrométrie Nucléaire et de Spectrométrie de Masse in Orsay.[13] The energy resolution was $\sim$15 keV, corresponding to a depth resolution of $\sim$10 nm. The analysis of the RBS spectra was made with the RUMP code.[14] The variations of the dimensions of the sample perpendicular to the ion beam direction were measured with an optical microscope.

## III. RESULTS AND DISCUSSION

Rutherford backscattering spectra recorded before and after irradiation at the maximum fluence of $3\times10^{13}$ at cm$^{-2}$ on three $Ni_3B/Au/Ni_3B$ sandwiches with a Au layer thickness $t_C$ of 300, 600, and 900 nm (the thickness $t_A$ of each of the $Ni_3B$ layers is 1 $\mu$m) are presented in Fig. 1. The signal characteristic of the backscattering of He ions on the Ni atoms of the front $Ni_3B$ layer corresponds to the large plateau starting at channel 390 and extending towards lower energies,[15] while the signal due to the backscattering of the analyzing particles on the Au atoms of the marker layer is represented by the peak situated between channels 170 and 350 (for the unirradiated samples). The position of the Au front edge, $f_C$, at the left of the Ni edge is due to the fact that the analyzing particles lose an important part of their energy in the front $Ni_3B$ layer before reaching the Au layer; the Au signal width, $w_C$, is directly related to the values of $t_C$. Irradiation with high-energy I ions has obviously led to different results depending on the initial thickness of the marker layer: a huge shift of $f_C$ towards higher energies, as well as a huge decrease of $w_C$ for the sample with $t_C=300$ nm [Fig. 1(a)]; nearly no change of the RBS parameters for the sample with $t_C=900$ nm [Fig. 1(c)]; an intermediate situation [smaller shift of $f_C$ and smaller de-

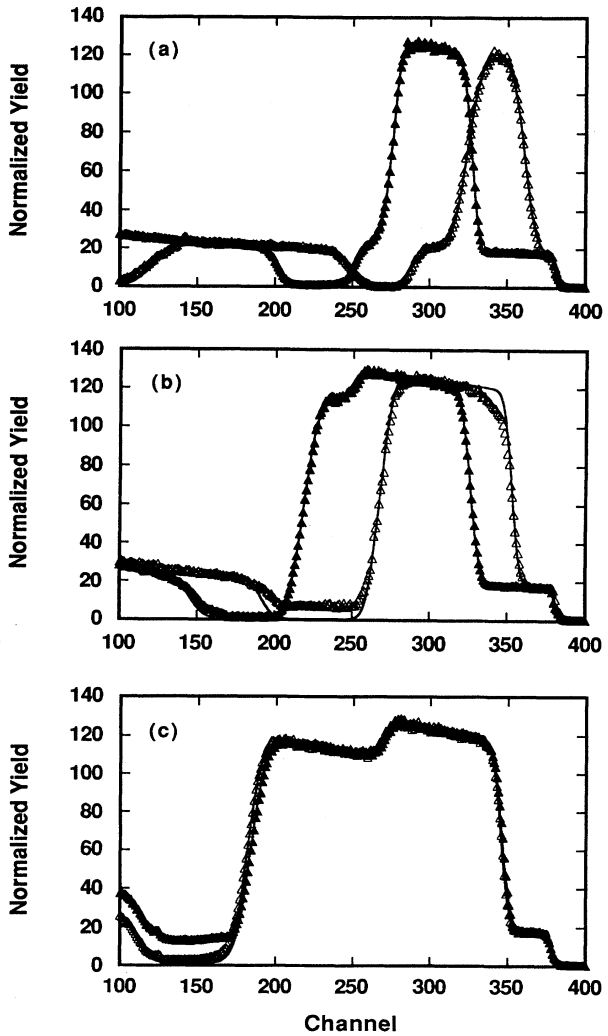


FIG. 1. RBS spectra recorded, before (filled triangles) and after (open triangles) irradiation at liquid nitrogen temperature with 500-MeV $^{127}I^{22+}$ ions (fluence: $3\times10^{13}$ at. cm$^{-2}$), on $Ni_3B/Au/Ni_3B$ sandwiches with a thickness of the $Ni_3B$ layers of 1 $\mu$m and three different thicknesses of the Au layer: (a) 300 nm, (b) 600 nm, and (c) 900 nm. Analyzing particles: 3.6-MeV $^4He^{2+}$ ions.

crease of $w_C$ than in the case of Fig. 1(a)] for the sample with $t_C = 600$ nm [Fig. 1(b)]. The shift of $f_C$ to high energy is due to the shrinkage of the front amorphous $Ni_3B$ layer, leading to a decrease of $t_A$,[16] and can be accounted for by the anisotropic growth of amorphous materials irradiated with swift heavy ions.[2-11] The decrease of $w_C$, which corresponds to a shrinkage of the Au layer (i.e., a decrease of $t_C$) is, at first glance, rather surprising owing to the fact that such an effect has never been evidenced in crystalline materials.[17] Therefore this shrinkage has to be attributed to the two adjacent and laterally expanding amorphous $Ni_3B$ layers. The most striking feature of the observed effect is that it concerns thicknesses of some hundreds of nanometers, i.e., quite bulky materials as compared to implanted samples for which the marker concentration is less than 2 at. %.[11]

Figure 2 presents the relative variations of $t_A$ and $t_C$ as a function of the I irradiation fluence for the three thicknesses of the Au layer represented in Fig. 1. This figure also includes the relative variations of the sample dimensions, $l$, perpendicular to the ion beam direction measured with the optical microscope. The data show that (i) the variations of $t_A$ and $t_C$ behave in the same way, irrespective of the amplitude of the effect; (ii) the sample dimensions perpendicular to the ion beam direction increase linearly with the ion fluence, while the thicknesses (parallel to the ion beam direction) of the various layers which compose the sandwiches decrease with a slope about twice higher, above a fluence threshold $\Phi_c$ of the order of $5\times10^{12}$ at. $cm^{-2}$; (iii) the thicker the crystalline layer buried in the amorphous matrix, the lower the amplitude of the changes of the dimensions of the various layers. In brief, these results demonstrate a similar quantitative behavior of the bulky crystalline layer with that of the amorphous one whatever their relative thicknesses. This similarity in the behavior under irradiation of the bulky crystalline layer and of the amorphous ones led us to describe the dimensional variations of the various layers which compose the sandwiches with the equations used for homogeneous amorphous materials[11]:

$$\frac{\Delta l_\perp}{l_{0\perp}} = \begin{cases} 0 & \text{if } \Phi \le \Phi_c \\ G(\Phi - \Phi_c) & \text{if } \Phi \ge \Phi_c \end{cases}, \tag{1}$$

$$\frac{\Delta l_\parallel}{l_{0\parallel}} = \begin{cases} 0 & \text{if } \Phi \le \Phi_c \\ \dfrac{1}{[1+G(\Phi-\Phi_c)]^2} - 1 & \text{if } \Phi \ge \Phi_c \end{cases}, \tag{2}$$

where $\Delta l_\perp / l_{0\perp}$ and $\Delta l_\parallel / l_{0\parallel}$ are the relative variations of the sample dimensions respectively perpendicular and parallel to the ion beam direction, $G$ is the growth rate, $\Phi$ is the ion fluence, and $\Phi_c$ is the incubation fluence. In our experiments, $\Delta l_\perp / l_{0\perp}$ is directly determined by optical microscopy, whereas $\Delta l_\parallel / l_{0\parallel}$ is measured on the different layers of the sandwiches via RBS.

The fits of Eqs. (1) and (2) to experimental data, which are represented by solid lines in Fig. 2, provide values of $G$ and $\Phi_c$ for the different experiments performed. It can be noted that the value of $G$ is strongly affected by the thickness of the Au layer, while the value of $\Phi_c$ is almost independent of $t_C$. In fact, a careful analysis of the whole set of data recorded on the $Ni_3B/Au/Ni_3B$ sandwiches shows that the relevant parameter is the ratio between the thicknesses of the crystalline and (total) amorphous layers $t_C/2t_A$. Figure 3 presents the variation of the growth rate with $t_C/2t_A$. The figure exhibits a rather regular decrease of the growth rate as $t_C/2t_A$ increases. Thus the presence of a sufficiently thick crystalline layer is able to hinder (and even to totally block) the plastic deformation of the amorphous part of the irradiated target. Moreover, a splitting seems to occur between the values of the growth rate determined by RBS or length measurements above $t_C/2t_A \sim 0.35$. Since RBS experiments sense the entire thickness of the sandwich layers while length measurements performed with the optical microscope are restricted to the surfaces of the samples, such a result could indicate a different physical behavior under irradiation between surface and bulk.[18]

As mentioned in the Introduction, when a swift heavy ion passes through a solid, it generates excitation and ionization of the target atoms along its path. It is now well established that these processes lead to damage creation whatever the structure of the target (crystalline or amorphous), and more specifically to anisotropic plastic deformation in amorphous materials. The mechanisms by which electronic excitation leads to atomic movements is still a matter of controversy: the various descriptions proposed are based either on the thermal spike concept,[19-20] the Coulomb explosion effect,[21-22] or the shock-wave phenomenon.[23] In the amorphous part of the

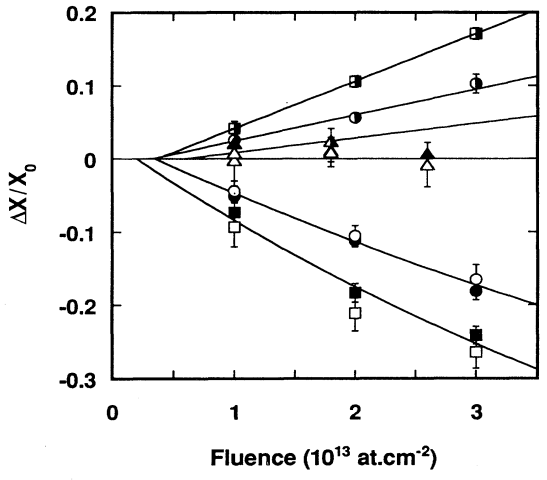


FIG. 2. Relative variation $\Delta X/X_0$ of $t_A$ (filled symbols), $t_C$ (open symbols) extracted from the analysis of RBS spectra, and 1 (half-filled symbols) measured by optical microscopy, as a function of the I irradiation fluence, for $Ni_3B/Au/Ni_3B$ sandwiches with three thicknesses of the Au layer: 300 nm (squares), 600 nm (circles), and 900 nm (triangles).

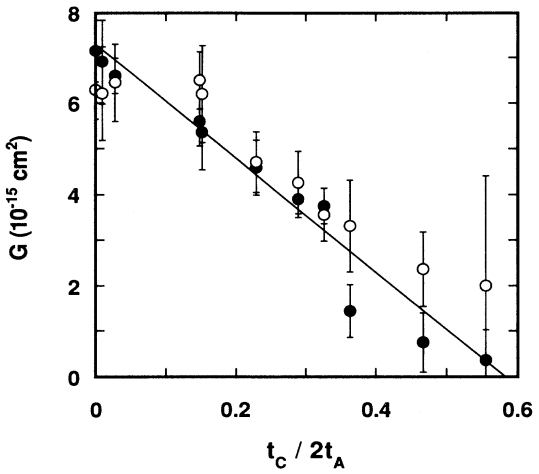


FIG. 3. Growth-rate $G$ extracted from RBS data (filled circles) and length measurements (open circles) as a function of the ratio between the thicknesses of the Au and $Ni_3B$ layers, $t_C/2t_A$, of $Ni_3B$/Au/$Ni_3B$ sandwiches. The solid line is a fit to RBS data with Eq. (3).

irradiated sandwiches, it is clear that the anisotropic growth is directly caused (as in the case of a homogeneous amorphous target) by ion irradiation. On the other hand, in the crystalline layer the growth is not directly linked to the passage of the incoming ions,[17] but is enforced by the deformation of the amorphous layers via the creation of a tensile stress $\sigma_C$ in the Au layer. Stress balance demands a corresponding compressive stress in the amorphous layers, which hinders the unperturbed growth of the latter ones. For the explanation of the relative dimensional changes observed in the various layers of the irradiated sandwiches, we use a simple rheological approach. The amorphous regions are assumed to obey Newtonian flow[24,25] with a strain rate $\dot{\epsilon}=G\varphi$ which lies between $10^{-5}$ and $10^{-7}$ $s^{-1}$, depending on $t_C/2t_A$. Far from the specimen surface, the contiguity of the sandwich layers demands the same strain rate for the Au layer. The constant value of $\dot{\epsilon}$ beyond $\Phi_c$, the temperature of 80 K, and the small size of the grains in the Au layer (lower than $t_C$) suggest that deformation occurs by a defectless flow mechanism, i.e., crystal planes are shifted against each other. This implies that the critical shear stress approximates the ideal shear strength: $\tau_C \sim 0.06\mu$ ($\mu$ is the shear modulus) which is virtually independent of $\dot{\epsilon}$.[26] Thus the stress balance in the sandwich layers yields for the variation of the growth rate with the thickness ratio $t_C/2t_A$

$$G=G_0\left[1+\frac{\sigma_c}{\sigma_\perp}\frac{t_c}{2t_a}\right], \tag{3}$$

where $G_0$ is the growth rate in the absence of the marker layer, and $\sigma_\perp$ denotes the biaxial compressive stress which hampers the straining in the amorphous part of the sample. The fit of Eq. (3) to experimental RBS data, which is represented by the full line in Fig. 3, provides values of $G_0=(7.2\pm0.3)\times10^{-15}$ $cm^2$ and $\sigma_C/\sigma_\perp=-1.7\pm0.4$. It is worth noting that the value of $G_0$ extracted from the present experiments is in good agreement with that obtained in similar measurements where the marker consisted of dilute Bi implanted atoms.[11] Using a shear modulus $\mu$ for Au at 80 K of 26.6 GPa, we obtain $\sigma_C=2.8$ GPa and $\sigma_\perp=-1.6$ GPa.

In amorphous materials, it is now well established that swift-heavy-ion irradiation generates anisotropic plastic flow which proceeds macroscopically as if the target would be submitted to a tensile mechanical stress perpendicular to the ion-beam direction. In fact, this deformation is not homogeneous at a microscopic scale, since it results from individual ion impacts. More precisely, each ion is supposed to create simultaneously radiation damage (here, free volume) in the core of its track and a transient radial shear stress around its path.[4–7] Inside the regions containing an excess of free volume, this stress triggers irreversible shear transformations leading to local plastic deformation. From a rheological point of view, the resulting deformation of the whole solid can be accounted for by an equivalent macroscopic tensile stress perpendicular to the beam direction and producing the same effect as the beam at a macroscopic level. In fully crystalline materials, an irradiating ion also creates disorder[27] in the core of its track and, likely, a similar transient shear stress which is not sufficiently intense to induce detectable plastic deformation, even after an accumulation of a great number of ion impacts. The rheological approach used to describe the behavior of the sandwiches, and which leads to Eq. (3), contains two parameters: the unperturbed growth rate $G_0$ and the compressive stress $\sigma_\perp$ preventing the growth in amorphous $Ni_3B$. From a microscopic point of view both arise from the mobility of the target atoms in the wake of the projectile ions. A recent model based on the thermal spike concept[28] could provide a way to understand the microscopic mechanisms which are represented phenomenologically by $G_0$ and $\sigma_\perp$.

## IV. CONCLUSION

The main result obtained from the experiments reported in this paper is the observation of a radiation-induced creep experienced by a thick crystalline layer embedded in an amorphous matrix during irradiation with swift heavy ions. Such a phenomenon does not occur in fully crystalline materials, i.e., without the presence of the amorphous substrate. It is due to the plastic deformation process occurring in the amorphous layers of the target, and it is induced by electronic excitation.

More precisely, as discussed above the amorphous layers behave under irradiation as if they were submitted to a macroscopic tensile stress perpendicular to the beam direction. Equilibrium conditions in the sandwich imply that the crystalline layer is also affected over long distances by the creation of a macroscopic tensile stress which can reach a magnitude comparable to that of the yield stress. The result is the creep of the crystalline ma-

terial. These considerations allowed us to develop a rheological model which reproduces the experimental results quite satisfactorily and provides an estimate of the equivalent global stress induced by an energetic ion beam in an amorphous solid.

## ACKNOWLEDGMENTS

We want to express our gratitude to the VICKSI and ARAMIS staffs for their assistance during irradiation and RBS analysis.

[1]R. L. Fleischer, P. B. Price, and R. M. Walker, *Nuclear Tracks in Solids* (University of California Press, Berkeley, 1975); B. E. Fischer and R. Spohr, Rev. Mod. Phys. **55**, 907 (1983).

[2]See the *Proceedings of the International Conference on Swift Heavy Ions in Matter* [Radiat. Eff. Def. Sol. **126**, 93 (1993)].

[3]S. Klaumünzer and G. Schumacher, Phys. Rev. Lett. **51**, 1987 (1983).

[4]S. Klaumünzer, Ming-dong Hou, and G. Schumacher, Phys. Rev. Lett. **57**, 850 (1986).

[5]S. Klaumünzer, Radiat. Eff. Def. Sol. **110**, 79 (1989).

[6]Ming-dong Hou, S. Klaumünzer, and G. Schumacher, Phys. Rev. B **41**, 1144 (1990).

[7]A. Benyagoub and S. Klaumünzer, Radiat. Eff. Def. Sol. **126**, 105 (1993).

[8]A. Audouard, E. Balanzat, G. Fuchs, J. C. Jousset, D. Lesueur, and L. Thomé, Europhys. Lett. **3**, 327 (1987); **5**, 241 (1988).

[9]A. Audouard, E. Balanzat, J. C. Jousset, A. Chamberod, G. Fuchs, D. Lesueur, and L. Thomé, Philos. Mag. B **63**, 727 (1991).

[10]A. Audouard, E. Balanzat, J. C. Jousset, D. Lesueur, and L. Thomé, J. Phys. Condens. Matter **5**, 995 (1993).

[11]L. Thomé, F. Garrido, J. C. Dran, A. Benyagoub, S. Klaumünzer, and A. Dunlop, Phys. Rev. Lett. **68**, 808 (1992).

[12]W. Busse, Nucl. Instrum. Methods A **293**, 103 (1990).

[13]E. Cottereau, J. Camplan, J. Chaumont, R. Meunier, and H. Bernas, Nucl. Instrum. Methods B **45**, 293 (1990).

[14]L. R. Doolittle, Nucl. Instrum. Methods B **9**, 344 (1985).

[15]The backscattering of the analyzing ions on the Ni atoms situated in the back (with respect to the ion beam direction) $Ni_3B$ layers provides a signal starting at channels 200, 150, and 100 (for unirradiated samples containing 300, 600, and 900 nm-thick Au layers, respectively) and extending far beyond the edge of the figure.

[16]It is worth noting that the back amorphous $Ni_3B$ layer experiences a similar shrinkage which cannot be measured with a good accuracy due to the great depth to be analyzed.

[17]S. Klaumünzer, Changlin Li, S. Löffler, M. Rammensee, G. Schumacher, and H. Neitzert, Radiat. Eff. Def. Sol. **108**, 131 (1989).

[18]Specific experiments on identical sandwiches implanted with dilute marker atoms at the surface of the amorphous layer are in progress in order to quantify this effect.

[19]F. Seitz and J. S. Koehler, Solid State Phys. **2**, 305 (1956).

[20]M. Toulemonde, C. Dufour, and E. Paumier, Phys. Rev. B **46**, 14 362 (1992).

[21]R. L. Fleischer, P. B. Price, and R. M. Walker, J. Appl. Phys. **36**, 3645 (1965).

[22]D. Lesueur and A. Dunlop, Radiat. Eff. Def. Sol. **126**, 163 (1993).

[23]I. S. Bitensky and E. S. Parilis, Nucl. Instrum. Methods B **21**, 26 (1987).

[24]E. Snoeks, A. Polman, and C. A. Volkert, Appl. Phys. Lett. **65**, 2487 (1994).

[25]A. Gutzmann, S. Klaumünzer, and P. Meier, Phys. Rev. Lett. **74**, 2256 (1995).

[26]H. J. Frost and M. F. Ashby, *Deformation-Mechanism Maps*, (Pergamon, Oxford, 1982).

[27]A. Dunlop and D. Lesueur, Radiat. Eff. Def. Sol. **126**, 123 (1993).

[28]H. Trinkaus and A. I. Ryazanov (unpublished); H. Trinkaus, J. Nucl. Mater. **223**, 196 (1995).